





Cite this: DOI: 10.1039/d6sc00591h

 All publication charges for this article have been paid for by the Royal Society of Chemistry

# Phosphine-catalyzed $\beta$ -C(sp<sup>3</sup>)-H functionalization of cyclic amines *via* a halogen based frustrated radical pairs approach

Yukun Xie, Xiaodan Meng, Chenrui Liu, Jiaming Tan, Xiaoxiang Zhang, Zhuan Zhang,  Shicheng Dong\* and Taoyuan Liang \*

The precise functionalization of saturated nitrogen-containing heterocycles is a cornerstone of modern drug discovery. While strategies targeting the  $\alpha$ -C(sp<sup>3</sup>)-H bond are well-established, functionalization at the distal  $\beta$ -position remains a formidable challenge, typically plagued by harsh conditions and reliance on noble metals. Herein, we report a metal-free, phosphine-catalyzed strategy for the  $\beta$ -position C(sp<sup>3</sup>)-H functionalization of cyclic amines, enabled by a novel frustrated radical pairs (FRPs) mechanism. Guided by density functional theory (DFT) calculations, we identified a thermodynamically stable yet reactivity potent "spoke-shaped" adduct derived from tris(2,6-dimethoxyphenyl)phosphine as the key catalytic species. Unlike traditional frustrated Lewis pairs (FLPs) systems based on boron or aluminum, this halogen-based system operates *via* a single electron transfer (SET) pathway to overcome the kinetic barriers of bond activation. This protocol features broad functional group tolerance, enabling diverse transformations (including sulfuration and heteroarylation) under unified, mild conditions. Furthermore, the utility of this method is demonstrated through the late-stage modification of complex pharmaceutical agents, offering a robust platform for the synthesis of bioactive amine derivatives.

Received 21st January 2026  
Accepted 20th March 2026

DOI: 10.1039/d6sc00591h

rsc.li/chemical-science

## Introduction

Saturated cyclic amines, particularly the piperidine scaffold, represent a privileged structural motif in medicinal chemistry, appearing ubiquitously in FDA-approved therapeutics.<sup>1</sup> Prominent examples include the complement C5a receptor antagonist Avacopan, the Janus kinase inhibitor Xeljanz (Tofacitinib), the anticoagulant Apixaban, and the BTK inhibitor Imbruvica (Ibrutinib).<sup>2</sup> Consequently, the development of streamlined methods to functionalize these heterocyclic cores is of paramount importance to the pharmaceutical sciences.<sup>3</sup>

Historically, green synthetic strategies such as visible-light catalysis and electrocatalysis have enabled diverse functionalization of cyclic amines.<sup>4</sup> The functionalization of cyclic amines has relied heavily on the generation of iminium intermediates trapped by nucleophiles.<sup>5</sup> In contrast, complementary strategies utilizing electrophiles to access  $\beta$ -functionalized products remain significantly underdeveloped.<sup>6</sup> This disparity stems from intrinsic challenges: the electron-withdrawing nature of the nitrogen atom renders the  $\beta$ -

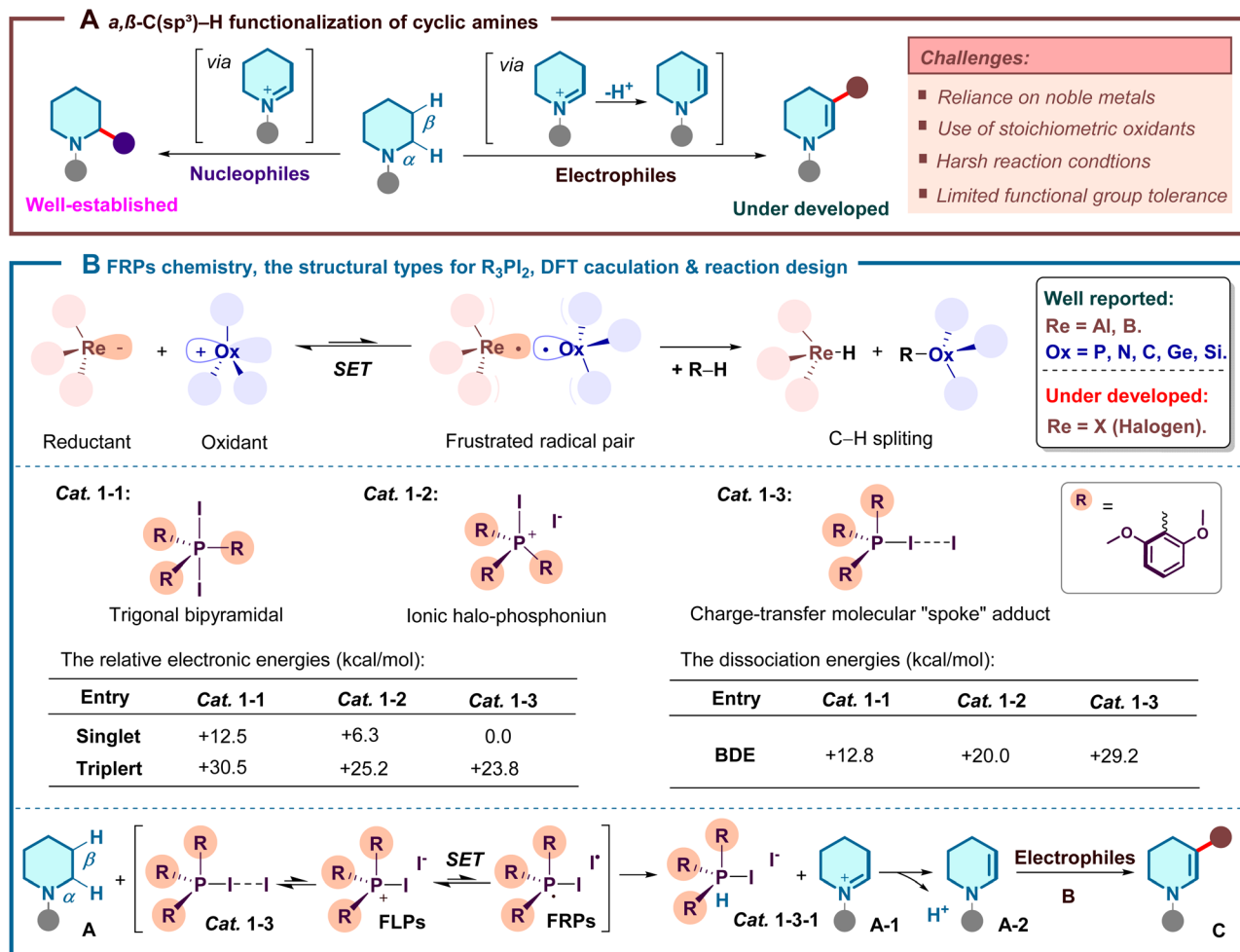
C(sp<sup>3</sup>)-H bond electron-deficient with a high bond dissociation energy (thermodynamic barrier), while the sterically accessible  $\alpha$ -position is kinetically favored.<sup>7</sup> Existing methods to overcome these hurdles often suffer from substantial limitations, including a reliance on noble metal catalysts, the use of stoichiometric oxidants, harsh reaction conditions, and limited functional group tolerance<sup>8</sup> (Scheme 1A). Therefore, the design of mild, metal-free systems capable of enabling electrophilic functionalization patterns remains a critical objective.

In recent years, frustrated Lewis pairs (FLPs) chemistry has evolved beyond ionic reactivity to encompass single electron transfer (SET) pathways, giving rise to the concept of frustrated radical pairs (FRPs).<sup>9</sup> By leveraging the equilibrium between a covalent adduct and a reactive radical pair (Re<sup>•</sup>/Ox<sup>•</sup>), these systems facilitate homolytic bond activation.<sup>10</sup> However, while FRPs systems based on aluminum/boron (Re = Al, B) and group 14/15 elements (Ox = P, N, C, Ge, Si) are well-established, halogen-based FRPs systems (Re = X) remain largely unexplored<sup>11</sup> (Scheme 1B, top). The development of a halogen-driven FRPs manifold could offer distinct reactivity profiles for activating inert C-H bonds.

Despite the long-standing recognition of triaryl halophosphine adducts, their synthetic utility remains underexploited relative to the broader field of organophosphorus chemistry.<sup>12</sup> Drawing inspiration from the three main structural

Guangxi Key Laboratory of Petrochemical Resource Processing and Process Intensification Technology, Guangxi Colleges and Universities Key Laboratory of Applied Chemistry Technology and Resource Development, School of Chemistry and Chemical Engineering, Guangxi University, Nanning, Guangxi 530004, P. R. China. E-mail: shicheng.dong@gxu.edu.cn; taoyuanliang@gxu.edu.cn





Scheme 1 Background and design of this work.

types of Ar<sub>3</sub>PI<sub>2</sub> adducts (*Cat. 1-1/1-2/1-3*), we hypothesized that such species could serve as ideal precursors for FRPs generation. Guided by DFT calculations (Scheme 1B, middle), we investigated the structural impact of substituents on the phosphorous center. The analysis revealed that the sterically congested and electron-rich tris(2,6-dimethoxyphenyl)phosphine forms a unique “spoke-shaped” diiodide adduct (Ar<sub>3</sub>PI<sub>2</sub>, Ar = 2,6-(MeO)<sub>2</sub>C<sub>6</sub>H<sub>3</sub>). This species (*Cat. 1-3*) is predicted to be the thermodynamically most stable isomer (0.0 kcal/mol) compared to its trigonal bipyramidal (*Cat. 1-1*) or ionic counterparts (*Cat. 1-2*). This unique electronic structure suggests that the Ar<sub>3</sub>PI<sub>2</sub> adduct can effectively mediate the formation of radical intermediates required for  $\beta$ -C(sp<sup>3</sup>)-H activation.

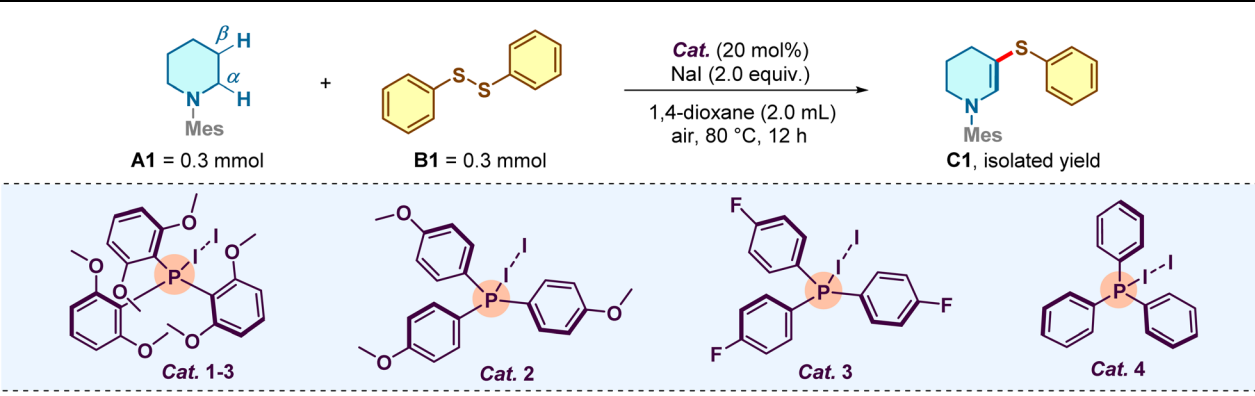
Based on these electronic features, we proposed a reaction design (Scheme 1B, bottom) wherein the specific “spoke-shaped” adducts *Cat. 1-3* serves as latent radical reservoirs, releasing transient FRPs *via* intramolecular SET, and they capable of overcoming the thermodynamic barrier of the  $\beta$ -C(sp<sup>3</sup>)-H bond, allowing for the direct coupling with electrophiles (**B**) to access functionalized products (**C**). Herein, we report a phosphine-catalyzed dehydrogenative functionalization of cyclic amines validated by this design. This strategy

obviates the need for transition metals or harsh oxidants, enabling the efficient construction of C-S or C-C bonds at the challenging  $\beta$ -position. The reaction features excellent scalability and broad functional group compatibility, providing a powerful tool for the late-stage diversification of drug molecules and complex natural products.

## Results and discussion

We commenced our investigation by selecting *N*-mesitylperidine (**A1**) and diphenyl disulfide (**B1**) as model substrates to validate our hypothesis. Encouragingly, exposing the mixture to catalytic amounts of *Cat. 1-3* (20 mol%) and NaI (2.0 equiv.) in 1,4-dioxane at 80 °C under an air atmosphere delivered the desired  $\alpha,\beta$ -dehydrogenative sulfuration product **C1** in 84% yield (Table 1, entry 1). With this promising lead result, we sought to verify the crucial role of the phosphine structure guided by our initial DFT calculations. Evaluation of a series of Ar<sub>3</sub>PI<sub>2</sub> adducts revealed a distinct structure-activity relationship (entries 2-4). While *para*-monosubstituted variants (*Cat. 2* and *Cat. 3*) maintained moderate catalytic efficacy, the removal of the *ortho*-methoxy groups (*Cat. 4*, unsubstituted



Table 1 Optimization of the reaction conditions<sup>a</sup>


Entry	Variation from standard conditions	Yield (%) <sup>b</sup>
1	None	84
2	<b>Cat. 2</b> instead of <b>Cat. 1-3</b>	77
3	<b>Cat. 3</b> instead of <b>Cat. 1-3</b>	73
4	<b>Cat. 4</b> instead of <b>Cat. 1-3</b>	21
5	Without <b>Cat. 1-3</b>	N.D.
6	10 mol% <b>Cat. 1-3</b>	72
7	25 mol% <b>Cat. 1-3</b>	83
8	Without NaI	62
9	I <sub>2</sub> instead of NaI	Trace
10	KI instead of NaI	74
11	NH <sub>4</sub> I instead of NaI	68
12	Ar instead of air	20
13	Toluene instead of 1,4-dioxane	65
14	CH <sub>3</sub> CN instead of 1,4-dioxane	26
15	DMF instead of 1,4-dioxane	17
16	DCE instead of 1,4-dioxane	Trace

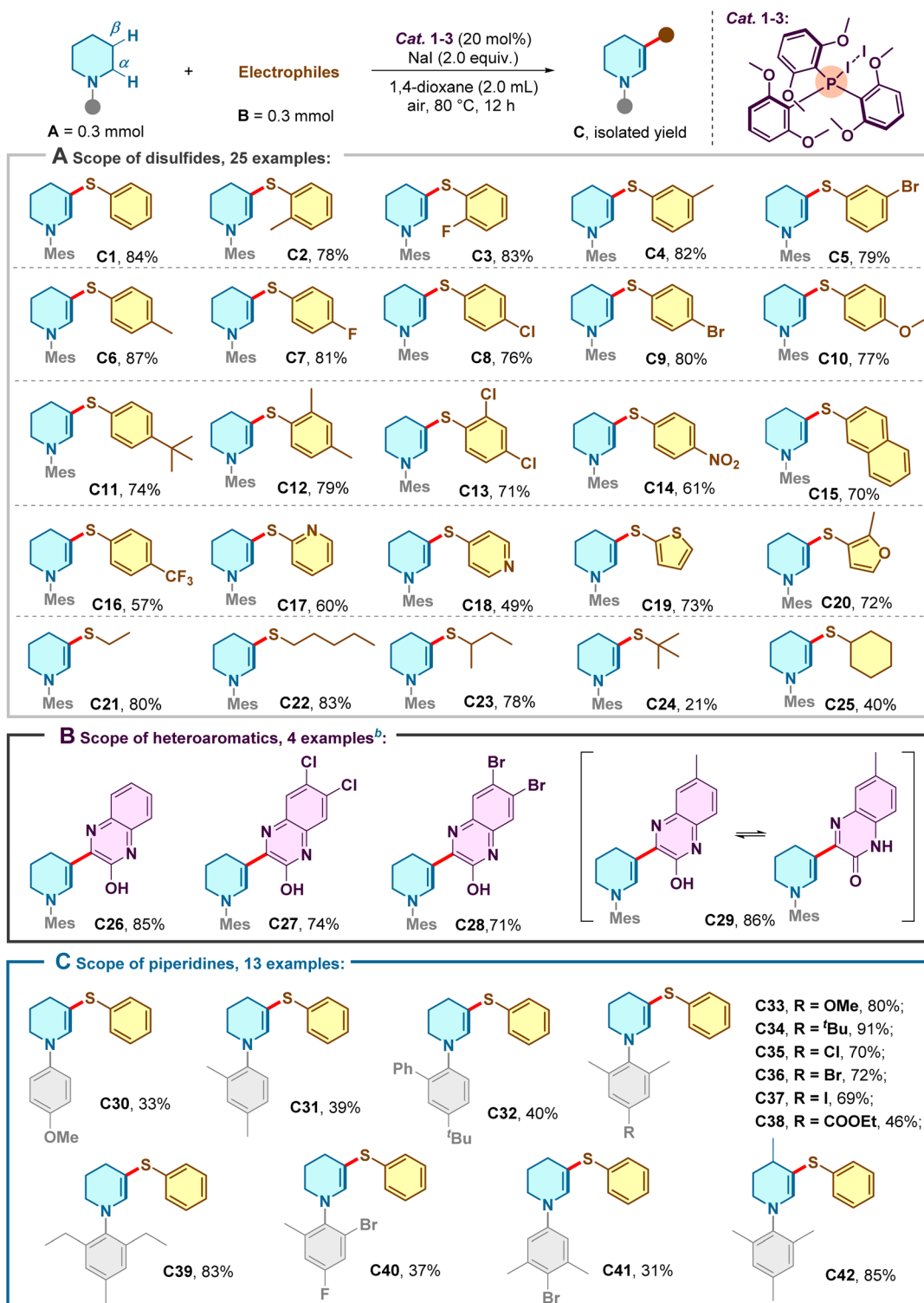
<sup>a</sup> Reaction conditions, unless specified otherwise: **A1** (0.3 mmol), **B1** (0.3 mmol), **Cat. 1-3** (0.06 mmol), NaI (0.6 mmol) and 1,4-dioxane (2.0 mL) were stirred under air atmosphere at 80 °C for 12 h. <sup>b</sup> Isolated yield. Mes = mesityl. DMF = *N,N*-dimethylformamide, DCE = 1,2-dichloroethane.

Ph<sub>3</sub>P) resulted in a precipitous drop in yield to 21%. This finding strongly supports our design rationale that the steric bulk and electron-donating capability of the 2,6-dimethoxyphenyl moiety are essential for stabilizing the active “spoke-shaped” charge-transfer complex (entry 5). Further optimization of reaction parameters indicated that the catalyst loading could not be reduced without compromising efficiency (entry 6), nor did increasing it provide further benefit (entry 7). Control experiments underscored the complexity of the iodine source: while the reaction proceeded in moderate yield without NaI (entry 8), the addition of external iodide significantly boosted efficiency, likely by facilitating the regeneration of the active iodine species. Notably, conducting the reaction under an argon atmosphere drastically inhibited the transformation (20% yield, entry 12), confirming the indispensable role of dioxygen as the terminal oxidant in the catalytic turnover. Ultimately, when other solvents were tested as replacements in the reaction, all of them performed less effectively than 1,4-dioxane (entries 13–16).

With the optimal conditions in hand, we evaluated the generality of this protocol (Scheme 2). The reaction exhibited remarkable tolerance toward the electronic properties of the

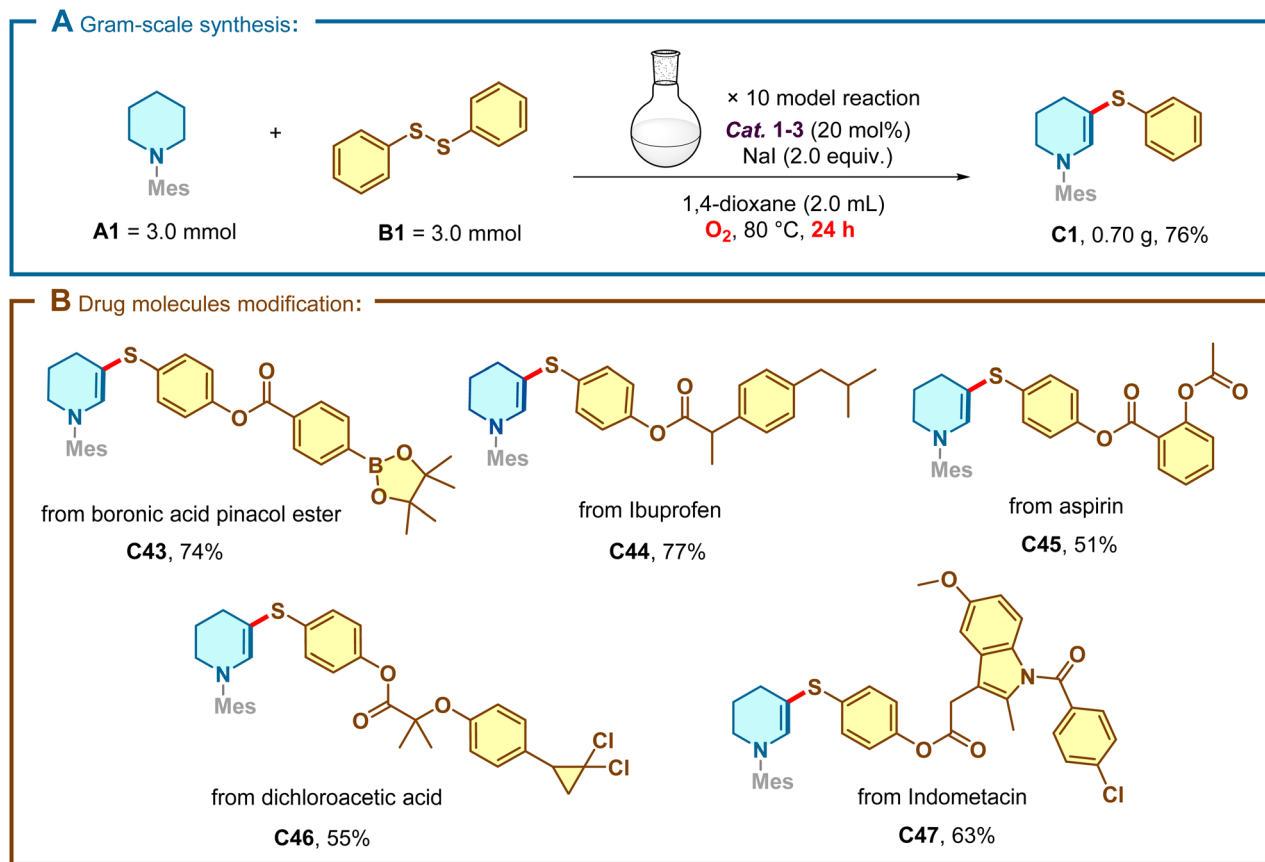
disulfide partners. Symmetrical diaryl disulfides bearing electron-donating (*e.g.*, –Me, –OMe) or weakly electron-withdrawing groups (*e.g.*, –F, –Cl, –Br) at various positions proceeded smoothly, delivering the target β-functionalized products in good to excellent yields (76–87%, **C1–C9**). Sterically demanding substrates, such as those containing *ortho*-substituents or a naphthyl backbone, were also accommodated efficiently (**C11–C15**). Notably, the system proved robust even with highly electron-deficient substrates, a challenging class for oxidative couplings. Disulfides bearing strong electron-withdrawing groups (–NO<sub>2</sub>, –CF<sub>3</sub>) or electron-deficient heteroarenes (pyridines) were successfully engaged, affording products **C16–C18** in useful yields. The scope further extended to heteroaryl disulfides derived from thiophene and furan (**C19–C20**) and, significantly, to aliphatic disulfides (**C21–C25**), demonstrating the versatility of this radical manifold beyond purely aromatic systems. Expanding the electrophile scope beyond sulfur, we demonstrated that 2-hydroxyquinoxalines serve as competent coupling partners, enabling a direct C–C bond-forming heteroarylation (Scheme 2B). Both electron-rich and electron-poor quinoxalines participated effectively (**C26–C28**). Interestingly, the reaction





Scheme 2 Scope of substrate. <sup>a</sup>Reaction conditions: cyclic amines A (0.3 mmol), electrophiles B (0.3 mmol), Cat. 1-3 (20 mol%), Nal (0.6 mmol), and 1,4-dioxane (2.0 mL) were stirred under air atmosphere at 80 °C for 12 h. <sup>b</sup>0.6 mmol of heteroaromatics were used.





Scheme 3 Gram-scale synthesis and drug molecules modification.

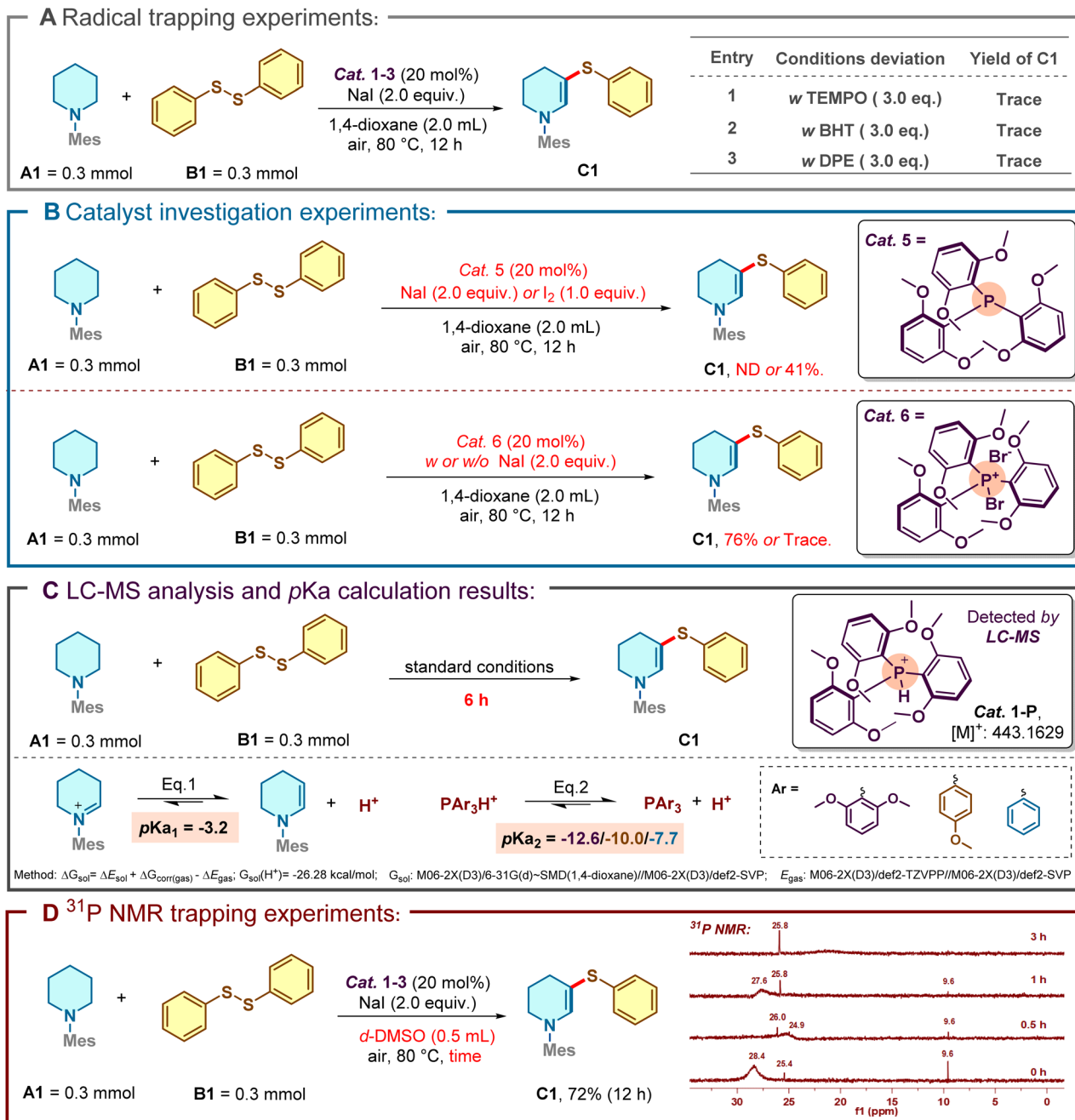
with a methyl-substituted substrate yielded the product as a tautomeric mixture (C29). Finally, variations on the piperidine skeleton were investigated (Scheme 2C). The protocol tolerated diverse substitution patterns on the *N*-aryl ring, including sterically congested 2,6-disubstituted systems (C30–C41). Substituents on the piperidine core itself were also compatible, as evidenced by the high yield of C42.

To underscore the practical utility of this methodology, a gram-scale synthesis was conducted (Scheme 3A). Under standard conditions with a prolonged reaction time (24 h), the model reaction was successfully scaled up to 3.0 mmol, furnishing 0.70 g of C1 (76% yield) without significant erosion of efficiency. Furthermore, the mildness of the protocol prompted us to explore the late-stage functionalization of complex bioactive molecules (Scheme 3B). Piperidine derivatives containing boronic esters or motifs derived from commercial pharmaceuticals, including ibuprofen, aspirin, dichloroacetic acid, and Indomethacin were all viable substrates (C43–C47). These results highlight the potential of this phosphine-catalyzed strategy as a powerful tool for accelerating structure–activity relationship (SAR) studies in medicinal chemistry.

To elucidate the operating mechanism, a series of control experiments were conducted (Scheme 4). (1) Radical trapping experiments: the addition of radical scavengers (TEMPO:

2,2,6,6-tetramethyl-1-piperidinyloxy, BHT: butylated hydroxytoluene, or DPE: stilbene) completely suppressed the product formation (Scheme 4A), strongly implicating the involvement of radical intermediates. (2) Catalytic active species identification: further investigation into catalyst efficacy revealed that triarylphosphine **Cat. 5** did not promote the reaction. In contrast, substitution of NaI with I<sub>2</sub> afforded the corresponding product C1 in 41% yield. These results suggest that Ar<sub>3</sub>PI<sub>2</sub> adducts, rather than the phosphine itself, serve as the active catalytic species (Scheme 4B, top). The critical role of the iodide anion was verified using the phosphonium bromide **Cat. 6**. Reaction efficiency was only observed when **Cat. 6** was combined with NaI (76% yield), whereas **Cat. 6** alone yielded only trace amounts of C1 (Scheme 4B, bottom). (3) LC-MS analysis of the reaction mixture after 6 hours under standard conditions revealed the characteristic fragment peak of Ar<sub>3</sub>PH<sup>+</sup>, but no ion fragment peak of Ar<sub>3</sub>P was observed. Meanwhile, we calculated the pK<sub>a</sub> values for the deprotonation of the iminium ion to form the enamine intermediate and the deprotonation of PAR<sub>3</sub>H<sup>+</sup>, respectively. A comparison of these two values revealed that pK<sub>a1</sub> (−3.2) was higher than pK<sub>a2</sub> (**Cat.1-3/Cat.2/Cat.4**: −12.6/−10.0/−7.7), indicating that the species in Eq. 2 possessed a stronger proton-donating ability. Thus, the deprotonation of the iminium ion to form the enamine *via* Eq. 2 is thermodynamically unfeasible, which





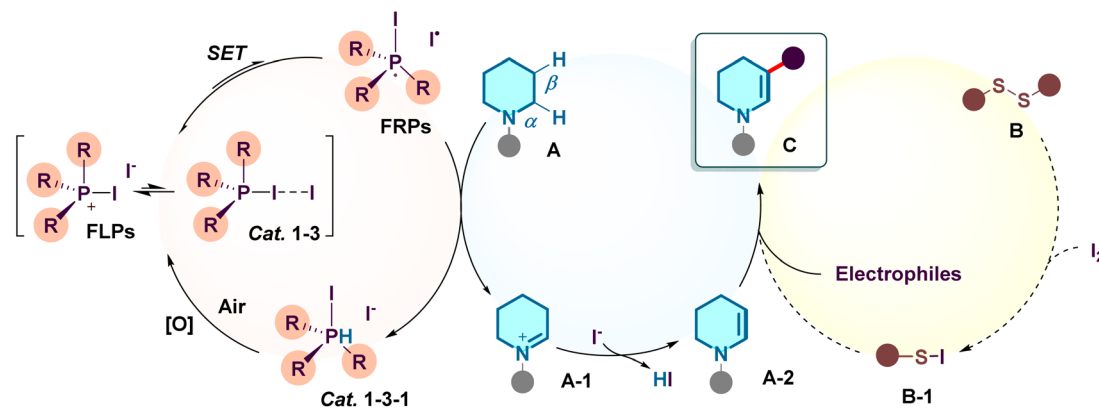
Scheme 4 Control experiments.

also indirectly confirms that no  $Ar_3P$  is generated in the catalytic cycle (Scheme 4C). (4)  $^{31}P$  NMR tracking experiments:  $^{31}P$  NMR monitoring of the reaction mixture revealed the involvement of the  $Ar_3PI_2$  species. As the reaction progressed, the complex signal pattern observed initially evolved into a distinct peak at  $\delta$  25.8 ppm, which persisted throughout the reaction course (Scheme 4D).

Proposed mechanism based on these experimental findings and literature precedents, a plausible catalytic cycle is depicted in Scheme 5. The reaction initiates with the formation of the spoke-shaped adduct **Cat. 1-3**, which undergoes homolytic

cleavage (or SET) to generate the FRPs species (containing a phosphine radical cation and an iodine radical). This potent FRPs intermediate mediates a hydrogen atom transfer (HAT) or SET process with the piperidine substrate **A** to generate the  $\beta$ -carbon radical or radical cation species. Subsequent dehydrogenation yields the enamine intermediate **A-2** (via iminium **A-1**), while the reduced catalyst species **Cat. 1-3-1** is re-oxidized by atmospheric oxygen to close the catalytic cycle. Finally, the *in situ* generated enamine **A-2** undergoes electrophilic interception by the electrophiles **B** (sulphur electrophiles could be





Scheme 5 Proposed reaction mechanism.

generated by the reaction of disulfides with elemental iodine) to deliver the final product C.

## Conclusions

In summary, we have developed a novel phosphine-catalyzed strategy for the regioselective  $\beta$ -C(sp<sup>3</sup>)-H functionalization of cyclic amines. This work represents a rare example of a halogen-based frustrated radical pair (FRP) system applied to organic synthesis. By rationally designing a sterically encumbered “spoke-shaped” P-I adduct, we successfully harnessed the reactivity of transient radicals to forge C-S and C-C bonds under mild, metal-free conditions. The protocol exhibits broad scope, excellent functional group tolerance, and high scalability, as demonstrated by the late-stage diversification of complex pharmaceutical agents. We anticipate that this distinct reaction design, leveraging the unique redox properties of group 15/17 adducts will inspire further developments in the activation of inert C-H bonds.

## Experiments and methods

### General information

All reactions were performed under air unless otherwise stated. All catalysts were synthesized following literature procedures. Full details of the experiments and methods employed in this study are listed in the accompanying SI.

### Typical procedure for the synthesis of C

Add electrophiles B (0.3 mmol), *Cat.* 1-3 (42 mg, 0.06 mmol), NaI (90 mg, 0.6 mmol), 1,4-dioxane (2.0 mL), and *N*-Mes piperidine A (0.3 mmol) sequentially into a reaction tube. Stir the mixture at 80 °C for 12 hours under an air. Concentrate the resulting mixture by removing the solvent under vacuum, then purify the residue *via* silica gel preparative thin-layer chromatography using petroleum ether as the eluent to obtain a colorless liquid C.

### Computational details

All the calculations were performed using the Gaussian 16 software package.<sup>13</sup> Geometry optimization of the compounds

was conducted at the M06-2X<sup>14</sup>(D3)<sup>15</sup> density functional theory level using the basis set def2-SVP<sup>10</sup> for all atoms. In addition, Hessian calculations for obtaining the vibrational frequencies were performed at the same level of theory as that for the geometry optimization to check whether the optimized geometrical structure is an energy minimum (with no imaginary frequency). The single-point energies calculations were performed by the M06-2X(D3) density functional with the def2-TZVPP for all atoms, and the CPCM solvent model<sup>16</sup> as used to simulate the solvent effect of 1,4-dioxane. Renderings of spin density plots were performed using the program VMD.<sup>17</sup>

## Author contributions

Y. Xie, X. Meng, C. Liu and J. Tan performed the experiments, collected and analyzed the data. Y. Xie wrote the original draft. X. Zhang and Z. Zhang assisted in revising the manuscript. S. Dong performed the DFT calculations. T. Liang conceived and directed the project, and revised the manuscript. All authors have given approval to the final version of the manuscript.

## Conflicts of interest

There are no conflicts to declare.

## Data availability

The data supporting this article have been included as part of the supplementary information (SI). Supplementary information: further information, including general experimental information, optimization studies, detailed experimental procedures, compound characterization data and NMR spectra of new compounds. See DOI: <https://doi.org/10.1039/d6sc00591h>.

## Acknowledgements

The authors thank the Guangxi Science and Technology Base and Talent Special Project (GuikeAD23026110), the Natural Science Foundation of Guangxi Province (2025GXNSFAA069929), Opening Project of Guangxi Key



Laboratory of Petrochemical Resource Processing and Process Intensification Technology (2025K007), the National Natural Science Foundation of China (22201048) and the Innovation Project of Guangxi Graduate Education (YCBZ2024010) for financial support.

## Notes and references

- (a) P. Hutani, G. Joshi, N. Raja, N. Bachhav, P. K. Rajanna, H. Bhutani, A. T. Paul and R. Kumar, U.S. FDA Approved Drugs from 2015–June 2020: A Perspective, *J. Med. Chem.*, 2021, **64**, 2339; (b) E. Vitaku, D. T. Smith and J. T. Njardarson, Analysis of the Structural Diversity, Substitution Patterns, and Frequency of Nitrogen Heterocycles among U.S. FDA Approved Pharmaceuticals, *J. Med. Chem.*, 2014, **57**, 10257; (c) C. M. Marshall, J. G. Federice, C. N. Bell, P. B. Cox and J. T. Njardarson, An Update on the Nitrogen Heterocycle Compositions and Properties of U.S. FDA-Approved Pharmaceuticals (2013–2023), *J. Med. Chem.*, 2024, **67**, 11622; (d) R. D. Taylor, M. MacCoss and A. D. G. Lawson, Rings in Drugs, *J. Med. Chem.*, 2014, **57**, 5845; (e) G. A. Aleku, Imine Reductases and Reductive Aminases in Organic Synthesis, *ACS Catal.*, 2024, **14**, 14308.
- (a) D. R. W. Jayne, P. A. Merkel, T. J. Schall, P. Bekker and A. S. Group, Avacopan for the Treatment of ANCA-Associated Vasculitis, *N. Engl. J. Med.*, 2021, **384**, 599; (b) E. B. Lee, R. Fleischmann, S. Hall, B. Wilkinson, J. D. Bradley, D. Gruben, T. Koncz, S. Krishnaswami, G. V. Wallenstein, C. Zang, S. H. Zwillich, R. F. van Vollenhoven and O. S. Investigators, Tofacitinib versus methotrexate in rheumatoid arthritis, *N. Engl. J. Med.*, 2014, **370**, 2377; (c) S. Mitsuboshi, K. Hayakawa, H. Hamano, A. Oshima, T. Takeda, K. Murakawa, H. Mori and Y. Zamami, Influence of vasopressin receptor antagonists on triple-whammy acute kidney injury: A VigiBase analysis, *Br. J. Clin. Pharmacol.*, 2024, **90**, 900.
- (a) M. Arisawa, S. Ohno, M. Miyoshi and K. Murai, Non-Directed  $\beta$ - or  $\gamma$ -C(sp<sup>3</sup>)-H Functionalization of Saturated Nitrogen-Containing Heterocycles, *Synthesis*, 2021, **53**, 2947; (b) Y. He, Z. Zheng, J. Yang, X. Zhang and X. Fan, Recent advances in the functionalization of saturated cyclic amines, *Org. Chem. Front.*, 2021, **8**, 4582; (c) W. Sun, A. Liao, L. Lei, X. Tang, Y. Wang and J. Wu, Research progress on piperidine-containing compounds as agrochemicals, *Chin. Chem. Lett.*, 2025, **36**, 109855; (d) J. W. Greenwood, M. A. Larsen, S. A. Burgess, J. A. Newman, Y. Jiang and A. Sather, Isolable iminium ions as a platform for N-(hetero)aryl piperidine synthesis, *Nat. Synth.*, 2023, **2**, 1059; (e) S. Park, G. Kang, C. Kim, D. Kim and S. Han, Collective total synthesis of C4-oxygenated securinine-type alkaloids via stereocontrolled diversifications on the piperidine core, *Nat. Commun.*, 2022, **13**, 5149; (f) C. Le, Y. Liang, R. W. Evans, X. Li and D. W. C. MacMillan, Selective sp<sup>3</sup> C-H alkylation via polarity-match-based cross-coupling, *Nature*, 2017, **547**, 79.
- (a) B. McManus, N. P. R. Onuska and D. A. Nicewicz, Generation and alkylation of  $\alpha$ -carbonyl radicals via organic photoredox catalysis, *J. Am. Chem. Soc.*, 2018, **140**, 9056; (b) L. F. T. Novaes, J. S. K. Ho, K. Mao, E. Villemure, J. A. Terrett and S. Lin,  $\alpha,\beta$ -Desaturation and formal  $\beta$ -C(sp<sup>3</sup>)-H fluorination of N-substituted amines: a late-stage functionalization strategy enabled by electrochemistry, *J. Am. Chem. Soc.*, 2024, **146**, 22982; (c) W. Lu, Z. Liu, Z. Liao, Z. Gao, K. Chen, H. Xiang and H. Yang, Photoinduced Pd-catalyzed formal asymmetric allylic substitution of piperidine scaffolds, *ACS Catal.*, 2025, **15**, 4384–4393; (d) T. Feng, S. Wang, Y. Liu, S. Liu and Y. Qiu, Electrochemical desaturative  $\beta$ -acylation of cyclic N-aryl amines, *Angew. Chem., Int. Ed.*, 2022, **61**, e202115178.
- (a) J. W. Rackl, A. F. Müller, A. Profyllidou and H. Wennemers, Regiodivergent  $\alpha$ - and  $\beta$ -Functionalization of Saturated N-Heterocycles by Photocatalytic Oxidation, *J. Am. Chem. Soc.*, 2025, **147**, 23381; (b) J. W. Greenwood, M. A. Larsen, S. A. Burgess, J. A. Newman, Y. Jiang and A. C. Sather, Isolable iminium ions as a platform for N-(hetero)aryl piperidine synthesis, *Nat. Synth.*, 2023, **2**, 1059; (c) R. C. Phillips, J. C. K. Chu, A. A. Rafaniello and M. J. Gaunt, Selective endo-Cyclic  $\alpha$ -Functionalization of Saturated N-Alkyl Piperidines, *J. Org. Chem.*, 2025, **90**, 12226.
- (a) X. Sheng, M. Yan, B. Zhang, W.-Y. Wong, N. Kambe and R. Qiu, Nickel-Catalyzed Site-Selective C3-H Functionalization of Quinolines with Electrophilic Reagents at Room Temperature, *ACS Catal.*, 2023, **13**, 9753; (b) T. Feng, S. Wang, Y. Liu, S. Liu and Y. Qiu, Electrochemical Desaturative  $\beta$ -Acylation of Cyclic N-Aryl Amines, *Angew. Chem., Int. Ed.*, 2022, **61**, e202115178; (c) P. J. Sarver, V. Bacauanu, D. M. Schultz, D. A. DiRocco, Y. H. Lam, E. C. Sherer and D. W. C. MacMillan, The merger of decatungstate and copper catalysis to enable aliphatic C(sp<sup>3</sup>)-H trifluoromethylation, *Nat. Chem.*, 2020, **12**, 459; (d) X. Meng, Y. Xie, P. Liu, X. Li, X. Zhang, Z. Zhang and T. Liang, Transition metal-free  $\alpha,\beta$ -C(sp<sup>3</sup>)-H dehydrogenative diazotization of piperidines under mild conditions, *Green Chem.*, 2026, **28**, 2694.
- D. Wayner, K. Clark, A. Rauk, D. Yu and D. Armstrong, C–H Bond Dissociation Energies of Alkyl Amines: Radical Structures and Stabilization Energies, *J. Am. Chem. Soc.*, 1997, **119**, 8925.
- (a) W. Hen, L. Ma, A. Paul and D. Seidel, Direct  $\alpha$ -C-H Bond Functionalization of Unprotected Cyclic Amines, *Nat. Chem.*, 2018, **10**, 165; (b) J. E. Spangler, Y. Kobayashi, P. Verma, D.-H. Wang and J.-Q. Yu,  $\alpha$ -Arylation of Saturated Azacycles and N-Methylamines via Palladium(II)-Catalyzed C(sp<sup>3</sup>)-H Coupling, *J. Am. Chem. Soc.*, 2015, **137**, 11876; (c) K. Moriya and P. Knochel, Diastereoconvergent Negishi Cross-Coupling Using Functionalized Cyclohexylzinc Reagents, *Org. Lett.*, 2014, **16**, 924; (d) P. Verma, J. M. Richter, N. Chekshin, J. X. Qiao and J.-Q. Yu, Iridium(I)-Catalyzed  $\alpha$ -C(sp<sup>3</sup>)-H Alkylation of Saturated Azacycles, *J. Am. Chem. Soc.*, 2020, **142**, 5117; (e) X. Li, Z. Cheng, J. Liu, Z. Zhang,



- S. Song and N. Jiao, Selective Desaturation of Amides: A Direct Approach to Enamides, *Chem. Sci.*, 2022, **13**, 9056.
- 9 (a) A. Dasgupta, E. Richards and R. L. Melen, Frustrated Radical Pairs: Insights from EPR Spectroscopy, *Angew. Chem., Int. Ed.*, 2021, **60**, 53; (b) Z. Lu, M. Ju, Y. Wang, J. M. Meinhardt, J. I. Martinez Alvarado, E. Villemure, J. A. Terrett and S. Lin, Regioselective aliphatic C-H functionalization using frustrated radical pairs, *Nature*, 2023, **619**, 514; (c) S. Roediger, E. Le Saux, P. Boehm and B. Morandi, Coupling of unactivated alkyl electrophiles using frustrated ion pairs, *Nature*, 2024, **636**, 108; (d) G. C. Welch, R. R. San Juan, J. D. Masuda and D. W. Stephan, Reversible, Metal-Free Hydrogen Activation, *Science*, 2006, **314**, 1124.
- 10 (a) Z. Hu, Z. Cheng and N. Jiao, Organic Synthesis through Radical Innovation: Frustrated Radical Pairs, *Chin. J. Chem.*, 2024, **42**, 1157; (b) Z. Dong, H. H. Cramer, M. Schmidtman, L. A. Paul, I. Siewert and T. Muller, Evidence for a Single Electron Shift in a Lewis Acid-Base Reaction, *J. Am. Chem. Soc.*, 2018, **140**, 15419.
- 11 (a) S. Li, C. Hu, X. Cui, J. Zhang, L. L. Liu and L. Wu, Site-Fixed Hydroboration of Terminal and Internal Alkenes using BX<sub>3</sub>/(i)Pr<sub>2</sub>NET, *Angew. Chem., Int. Ed.*, 2021, **60**, 26238; (b) Y. Soltani, A. Dasgupta, T. A. Gazis, D. M. C. Ould, E. Richards, B. Slater, K. Stefkova, V. Y. Vladimirov, L. C. Wilkins, D. Willcox and R. L. Melen, Radical Reactivity of Frustrated Lewis Pairs with Diaryl Esters, *Cell Rep. Phys. Sci.*, 2020, **1**, 100016; (c) Y. Aramaki, N. Imaizumi, M. Hotta, J. Kumagai and T. Ooi, Exploiting single-electron transfer in Lewis pairs for catalytic bond-forming reactions, *Chem. Sci.*, 2020, **11**, 4305; (d) F. Xie, J. He and Y. Zhang, Frustrated-radical-pair-initiated atom transfer radical addition of perfluoroalkyl halides to alkenes, *Org. Chem. Front.*, 2023, **10**, 3861; (e) M. Wang, M. Shanmugam, E. J. L. McInnes and M. P. Shaver, Light-Induced Polymeric Frustrated Radical Pairs as Building Blocks for Materials and Photocatalysts, *J. Am. Chem. Soc.*, 2023, **145**, 24294.
- 12 (a) N. A. Barnes, S. M. Godfrey, R. Z. Khan, A. Pierce and R. G. Pritchard, A structural and spectroscopic study of tris-aryl substituted R<sub>3</sub>PI<sub>2</sub> adducts, *Polyhedron*, 2012, **35**, 31; (b) Q. Ma, Y. Shi and D. Wang, Phosphonium Salt-Promoted C2-H Functionalization of Heterocyclic N-Oxides, *Org. Lett.*, 2023, **25**, 9181; (c) G. R. F. Orton, B. S. Pilgrim and N. R. Champness, The chemistry of phosphines in constrained, well-defined microenvironments, *Chem. Soc. Rev.*, 2021, **50**, 4411; (d) R. H. Beddoe, K. G. Andrews, V. Magné, J. D. Cuthbertson, J. Saska, A. L. Shannon-Little, S. E. Shanahan, H. F. Sneddon and R. M. Denton, Redox-neutral organocatalytic Mitsunobu reactions, *Science*, 2019, **365**, 910; (e) M. Fu, R. Shang, B. Zhao, B. Wang and Y. Fu, Photocatalytic decarboxylative alkylations mediated by triphenylphosphine and sodium iodide, *Science*, 2019, **363**, 1429; (f) J. Feng, L. Nicchio, L. Liu, Y. Wu, K. Lu, S. Protti and X. Zhao, Recent advances in visible light-driven phosphine-mediated transformations, *Org. Chem. Front.*, 2025, **12**, 1695; (g) A. Noble and V. K. Aggarwal, Triphenylphosphine and sodium iodide: a new catalyst combination to rival precious metal complexes in visible light photoredox catalysis, *Sci. China Chem.*, 2019, **62**, 1083; (h) J. Sun, J. Xie, W. Lin and J. Li, Visible-light-induced direct photolysis of phosphorus iodide salts for difluoroalkylation of C(sp<sup>2</sup>)-H by an intramolecular charge-transfer complex, *Org. Lett.*, 2025, **27**, 11182.
- 13 F. M. J. Frisch, G. W. Trucks, H. B. Schlegel, G. E. Scuseria, M. A. Robb, J. R. Cheeseman, G. Scalmani, V. Barone, B. Mennucci, G. A. Petersson, H. Nakatsuji, M. Caricato, X. Li, H. P. Hratchian, A. F. Izmaylov, J. Bloino, G. Zheng, J. L. Sonnenberg, M. Hada, M. Ehara, K. Toyota, R. Fukuda, J. Hasegawa, M. Ishida, T. Nakajima, Y. Honda, O. Kitao, H. Nakai, T. Vreven, J. A. Jr. Montgomery, J. E. Peralta, F. Ogliaro, M. Bearpark, J. J. Heyd, E. Brothers, K. N. Kudin, V. N. Staroverov, R. Kobayashi, J. Normand, K. Raghavachari, A. Rendell, J. C. Burant, S. S. Iyengar, J. Tomasi, M. Cossi, N. Rega, J. M. Millam, M. Klene, J. E. Knox, J. B. Cross, V. Bakken, C. Adamo, J. Jaramillo, R. Gomperts, R. E. Stratmann, O. Yazyev, A. J. Austin, R. Cammi, C. Pomelli, J. W. Ochterski, R. L. Martin, K. Morokuma, V. G. Zakrzewski, G. A. Voth, P. Salvador, J. J. Dannenberg, S. Dapprich, A. D. Daniels, O. Farkas, J. B. Foresman, J. V. Ortiz, J. Cioslowski and D. J. Fox, *Gaussian 16, Revision A.03*; Gaussian, Inc., Wallingford CT, 2016.
- 14 (a) Y. Zhao and D. G. Truhlar, Density functionals with broad applicability in chemistry, *Acc. Chem. Res.*, 2008, **41**, 157–167; (b) Y. Zhao and D. G. Truhlar, The M06 suite of density functionals for main group thermochemistry, thermochemical kinetics, noncovalent interactions, excited states, and transition elements: two new functionals and systematic testing of four M06-class functionals and 12 other functionals, *Theor. Chem. Acc.*, 2008, **120**, 215–241.
- 15 (a) S. Grimme, J. Antony, S. Ehrlich and H. Krieg, A consistent and accurate ab initio parameterization of density functional dispersion correction (DFT-D) for the 94 elements H-Pu, *J. Chem. Phys.*, 2010, **132**, 154104; (b) S. Grimme, S. Ehrlich and L. Goerigk, Effect of the damping function in dispersion corrected density functional theory, *J. Comput. Chem.*, 2011, **32**, 1456–1465.
- 16 G. Scalmani and M. J. Frisch, Continuous surface charge polarizable continuum models of solvation. I. General formalism, *J. Chem. Phys.*, 2010, **132**, 114110.
- 17 W. Humphrey, A. Dalke and K. Schulten, VMD: Visual molecular dynamics, *J. Mol. Graphics*, 1996, **14**, 33–38.

